Organic Electronics xxx (xxxx) 106513

Contents lists available at ScienceDirect

Organic Electronics

journal homepage: www.elsevier.com/locate/orgel

Printable biflourene based ultra-violet (UV) organic light-emitting electrochemical cells (OLECs) with improved device performance

Sasikumar Arumugam [a, b, *], Yi Li [a], James E. Pearce [b], Katie L. Court [a], Giacomo Piana [c], Edward H. Jackman [b], Oliver J. Ward [b], Martin D.B. Charlton [c], John Tudor [a], David C. Harrowven [b], Steve P. Beeby [a]

[a] Smart Electronics Material and Systems Research Group, School of Electronics and Computer Science, University of Southampton, Southampton, SO17 1BJ, UK
[b] School of Chemistry, University of Southampton, Southampton, SO17 1BJ, UK
[c] Sustainable Electronic Technologies Research Group, School of Electronics and Computer Science, University of Southampton, Southampton, SO17 1BJ, UK

ARTICLE INFO

Keywords:
Light emitting
Electrochemical cells
E-textiles
Ultraviolet emission
Wearable electronics
Smart fabrics

ABSTRACT

A series of printable UV emitting ionic bifluorene derivatives have been prepared incorporating pendent alkylimidazolium groups. Herein, we detail the synthesis of compounds and the methods used in device fabrication. We show how ink formulation is improved by increasing the solubility of the active bifluorene through extension of the alkyl chain length and switching the counter ion from PF_6^- to $CF_3SO_3^-$. We also show how organic light emitting electrochemical cells (OLECs) can be fabricated by spray coating to achieve an active layer with a thickness of ~150–200 nm, leading to working devices with a turn on voltage of around 6.5 V. This gives electroluminescent (EL) that peaks between 385 nm and 390 nm with a maximum EL emission intensity of 1.29 μW/cm^2. Thus, EL emission within the UV range has been demonstrated successfully with the synthesised molecules via spray coating onto glass slides.

1. Introduction

Light emitting textiles are primarily made by incorporating emissive yarns within standard textiles using conventional weaving processes [1]. However, this approach is limited to the available yarn geometries and simple patterns that are amenable to weaving. To overcome this, off-the-shelf light emitting diodes (LED) and electroluminescent (EL) strips can be sewn, glued, or attached into a woven textile [2]. However, these approaches require manual assembly so are unsuitable for mass production, and limited to bespoke, high-value applications. To address this limitation, flexible electroluminescence textiles fabricated by screen printing [3], slot die coating [4], inkjet and dispenser printing [5,6], have also been developed. These have thick inorganic emission layers with limited colours for emission. Their high porosity and the surface roughness of textiles generally prevents the high precision fabrication required for LED functional layer deposition as the thickness of each functional layer in an LED has a strict range requirement.

Solution processed light emitting electrochemical cells (LECs) have the potential to solve this problem, as the thickness of each LEC functional layers is not critical and multiple organic emission materials are available to achieve large area light emitting textiles. In 1995, Pei et al. reported the first LECs on glass [7], with a device consisting of an active layer composed of an organic light emitter and an inorganic salt, sandwiched between an anode and cathode [8,9]. Subsequently, many variations have been reported with active layers employing highly conjugated organic molecules [10], polymers (PLECs) [11,12], ionic transition-metal complexes (iTMC-LECs) [13,14], quantum dots [15] and perovskites [16]. The commercial polymer Super Yellow (SY) and the yellow-orange emitting cyclometalated iridium(III) complex $[Ir(ppy)_2(pbpy)][PF_6]$ [17] are currently regarded as the best performing organic and inorganic LECs in terms of stability and brightness [13]. The performance and deposition of SY OLECs on plastics [18] and textiles [19] has been demonstrated exhibiting uninterrupted operation for 57 days at a brightness of 100 cd/m^2 and an efficiency of 10 lm/W [20].

Recently, Merck have commercialized several poly(*p*-phenylene vinylene) (PPV) based polymers including SY and related green and blue emitting polymers as active materials. In addition, some reports have demonstrated the viability of small molecule OLECs for green, red, blue, and white emission devices [21–24]. In those cases, additional ion-transport materials, such as polyethylene oxide (PEO), and salts

* Corresponding author. Smart Electronics Material and Systems Research Group, School of Electronics and Computer Science, University of Southampton, Southampton, SO17 1BJ, UK.
E-mail address: s.arumugam@soton.ac.uk (S. Arumugam).

https://doi.org/10.1016/j.orgel.2022.106513
Received 1 October 2021; Received in revised form 25 March 2022; Accepted 26 March 2022
1566-1199/

such as $LiCF_3SO_3$, must be added to the active layer solution [25]. This increased complexity of the active layer can lead to phase separation, affecting device performance [26]. However, a few approaches avoid the use of these dedicated electrolyte materials in OLECs through the appropriate selection of core molecules and associated salts. These approaches illustrate thin film OLECs consisting of simple combinations of small molecule light emitting materials and associated dissolved salts. In this arrangement the ionic emitter itself also acts as an electrolyte to distribute the salt [27].

UV emission from OLECs based on a combination of small molecule and associated salts is of interest due to the ability of UV light emission to kill bacteria and viruses (ultraviolet germicidal irradiation UVGI) [28]. The ability to print UV OLEC's on a textile could, for example, be used in a smart bandage to treat infected wounds and to accelerate the healing process [29,30]. In addition, a textile colour change can be realized using the photochromic effect triggered by the UV emission from textiles [29]. Chen et al. reported the use of ionic 2,2-bifluorene **4a** in the preparation of OLECs with methylimidazolium moieties as pendant groups [31]. UV EL emission at 386 nm with maximum external quantum and power efficiencies of 0.15% and 1.06 mW/W was obtained. Poly(methyl methacrylate) (PMMA) was added to the active layer to improve the film quality and device operation. Although PMMA did not have an active role it reduced the leakage current and increased device efficiency. However, poor solubility of the ionic molecule led to an investigation of an alternative molecule design and synthesis.

In this paper we show how some simple modifications to the 2,2′-bifluorene **4a** developed by Chen et al. has achieved improved device performance as UV-OLECs. Moreover, the improved solubility of these analogues has made it possible to use ethanol as the solvent for spray coating formulation. Fabrication has been carried out by direct spray coating onto commercial pre-coated ITO glass slide substrates which were chosen for their simplicity of handing. Although the device configuration may vary LECs on glass and textile substrates, the optimized fabrication parameters will be compatible. Spray coating has been used in the textile industry for large area deposition of layers on to fabric rolls. This long-standing technique is an attractive non-vacuum based process that can deposit a uniformly distributed thin functional layer. It is a non-contact deposition process as opposed to, for example, screen printing, and is ideally suited to large-scale roll to roll (R2R) processes. In this work, we coupled spray coating with a pre-defined shadow mask to achieve a desired pattern [32]. Fig. 1 shows the masked spray coating technique, which was used to realise OLECs, and provides a route to scalability with potential for widespread adoption of this fabrication method in light emitting textiles.

2. Experimental section

2.1. Active molecules synthesis

2.1.1. General remarks

All air sensitive reactions were carried out under argon using flame dried apparatus. Reactions were monitored by TLC on Merck Silica Gel 60 Å F TLC plates and visualised with 254 nm UV followed by aqueous 1% $KMnO_4$ or CAMPH. Flash chromatography was performed under slight positive pressure on Sigma Aldrich 40–63 μm 60 Å 230–400 Å silica. Reaction and chromatography solvents were removed using a rotary evaporator equipped with a diaphragm pump. ^1H, ^{13}C and ^{19}F NMR spectroscopy was performed on a Bruker AV400 (400/100/376 MHz) spectrometer at 298 K in $CDCl_3$ or DMSO-d_6. Chemical shifts are quoted as δ values in ppm using residual solvent peaks as the reference. Coupling constants J are given in Hz and multiplicity is described as follows: s, singlet; d, doublet; t, triplet; q, quartet; quin, quintet; m, multiplet; br, broad. HRMS data were obtained using a Bruker APEX III FT-ICR-MS with samples run in HPLC grade methanol. Electrospray mass spectrometry was performed on a directly injected Waters quadrupole MSD using ESI + ionisation with MeOH as solvent. 2-Bromofluorene, potassium hydroxide, *N*-butylimidazole, *N*-hexylimidazole, *N*-octylimidazole, $Pd_2(dba)_3$, 2-dicyclohexylphosphino-2′,4′,6′-triisopropylbiphenyl (XPhos), potassium hexafluorophosphate (KPF_6) and potassium trifluoromethane sulfonate were supplied by Fluorochem; dichloromethane, $B_2(pin)_2$, potassium phosphate, *N*-methylimidazole, acetone, dioxane, chloroform and hexane were supplied by Sigma Aldrich. Tetrahydrofuran, hexane and pentane were all distilled from sodium benzophenone ketyl under argon.

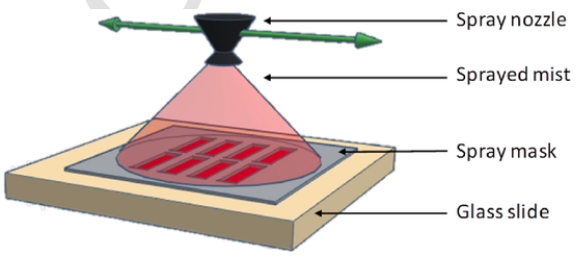

Fig. 1. Isometric pictorial representation of a single functional layer deposition by spray coating.

2.1.2. Procedures

2.1.2.1. 2-Bromo-9,9-bis-(6′-bromohexyl)fluorene, ***2****.* To a solution of potassium hydroxide (100 g, 1.78 mol) in water (200 mL), 2-bromofluorene (5.03 g, 20.5 mmol), TBAB (1.32 g, 4.09 mmol) and 1,6-dibromohexane (31.6 mL, 50.0 g, 205 mmol) was added. After heating to 70 °C for 18 h the reaction was cooled to RT, diluted with water (150 mL) and extracted with DCM (150 mL). The organic phase was separated, washed with dil. HCl (150 mL) and water (2 × 150 mL), dried over $MgSO_4$ and concentrated *in vacuo*. Purification by column chromatography (silica, 0–5% DCM in petrol) afforded the title compound **2** as a pale-yellow oil (7.00 g, 12.3 mmol, 60%). Data is consistent with literature values:[1] δ_H (400 MHz, $CDCl_3$) 7.68 (1H, m, Ar**H**), 7.56 (1H, m, Ar**H**), 7.50–7.43 (2H, m, Ar**H**), 7.38–7.29 (3H, m, Ar**H**), 3.29 (4H, t, J = 6.9 Hz, C**H**$_2$Br), 2.06–1.84 (4H, m, C**H**$_2$), 1.67 (4H, app. quin, J = 7.1 Hz, C**H**$_2$), 1.25–1.14 (4H, m, C**H**$_2$), 1.13–1.01 (4H, m, C**H**$_2$), 0.70–0.51 (4H, m, C**H**$_2$); δ_C (100 MHz, $CDCl_3$) 152.6 (**C**), 149.9 (**C**), 140.2 (**C**), 140.0 (**C**), 130.1 (**C**H), 127.6 (**C**H), 127.1 (**C**H), 126.0 (**C**H), 122.8 (**C**H), 121.1 (**C**H), 121.0 (**C**), 119.8 (**C**H), 55.2 (**C**), 40.1 (2 × **C**H$_2$), 33.9 (2 × **C**H$_2$), 32.6 (2 × **C**H$_2$), 29.0 (2 × **C**H$_2$), 27.7 (2 × **C**H$_2$), 23.5 (2 × **C**H$_2$); HRMS (APPI) $C_{25}H_{31}Br_3$ $[M]^+$ calculated 567.9970, observed 567.9971.

2.1.2.2. 9,9,9′,9′-Tetrakis-(6-bromohexyl)-9H,9′H-2,2′-bifluorene, ***3****.* To a solution of 2-bromofluorene **2** (501 mg, 0.877 mmol) in dioxane (5 mL) was added $B_2(pin)_2$ (114 mg, 0.448 mmol), potassium phosphate (560 mg, 2.64 mmol) and XPhos (9.0 mg, 19 μmol).[2] The solution was degassed by purging with argon, evacuating and backfilling with argon 3 times then $Pd_2(dba)_3$ (3.6 mg, 3.9 μmol) was added. After degassing a second time, the solution was heated at reflux for 6 h then water (0.5 mL) was added. After a further 22.5 h at reflux, the reaction was cooled to RT and extracted with DCM (20 mL). The organic phase was washed sequentially with H_2O (2 × 20 mL), HCl (2 M, 30 mL) and water (2 × 20 mL) then dried over $MgSO_4$, concentrated *in vacuo* and purified by column chromatography (silica, 20% DCM in petrol) to afford the title compound **3** as a white solid (288 mg, 0.293 mmol, 67%). Data is consistent with literature values:[1] δ_H (400 MHz, $CDCl_3$) 7.81 (2H, d, J = 7.8 Hz, Ar**H**), 7.75 (2H, br d, J = 7.5 Hz, Ar**H**), 7.66 (2H, br d, J = 7.8 Hz, Ar**H**), 7.62 (2H, s, Ar**H**), 7.42–7.30 (6H, m, Ar**H**), 3.28 (8H, t, J = 6.8, C**H**$_2$Br), 2.17–1.96 (8H, m, C**H**$_2$), 1.67 (8H, quin, J = 7.1 Hz, C**H**$_2$), 1.26–1.17 (8H, m, C**H**$_2$), 1.12 (8H, quin, J = 7.3 Hz, C**H**$_2$), 0.80–0.63 (8H, m, C**H**$_2$) ppm; δ_C (100 MHz, $CDCl_3$) 151.1 (2 × **C**), 150.6 (2 × **C**), 140.8 (2 × **C**), 140.44 (2 × **C**), 140.38

(2 × **C**), 127.1 (2 × **C**H), 127.0 (2 × **C**H), 126.2 (2 × **C**H), 122.8 (2 × C**H**), 121.2 (2 × **C**H), 120.0 (2 × **C**H), 119.8 (2 × **C**H), 55.1 (2 × **C**), 40.2 (4 × **C**H_2), 34.0 (4 × **C**H_2), 32.6 (4 × **C**H_2), 29.0 (4 × **C**H_2), 27.7 (4 × **C**H_2), 23.6 (4 × **C**H_2) ppm; HRMS (APPI) $C_{50}H_{62}Br_4$ $[M]^+$ calculated 978.1580, observed 978.1573.

2.1.2.3. 9,9,9′,9′-Tetrakis-(6-(1-methyl-3H-imidazolium-3-yl)hexyl)-9H,9′H-2,2′-bifluorene tetrakis(hexafluorophosphate), ***4a****.* A solution of bifluorene **3** (244 mg, 0.25 mmol) and *N*-methylimidazole (0.084 mL, 1.04 mmol) in toluene (20 mL) was heated at 100 °C for 18 h then cooled to RT and concentrated *in vacuo*. The resulting solid was dissolved in acetone (10 mL) and 1 M KPF_6 (10 mL) added. After 5 min the solution was concentrated *in vacuo*, then the resulting solid was washed with water (200 mL), dissolved in acetone (50 mL), concentrated *in vacuo*, washed with hexane (200 mL), dissolved in acetone (50 mL), concentrated *in vacuo* then sonicated under $CHCl_3$ (250 mL) for 15 min. The solid was collected by filtration, washed with further $CHCl_3$ (200 mL) then twice dissolved in acetone (50 mL) and concentrated *in vacuo* to afford the title compound **4a** as an off-white solid (339 mg, 0.22 mmol, 87%). Data is consistent with literature values:[1] δ_H (400 MHz, DMSO-d_6) 8.95 (4H, br s, 4 × Ar**H**), 7.89 (2H, d, J = 8.0 Hz, 2 × Ar**H**), 7.86–7.83 (4H, m, 4 × Ar**H**), 7.75 (2H, dd, J = 8.0, 1.4 Hz, 2 × Ar**H**), 7.62 (4H, t, J = 1.8 Hz, 4 × Ar**H**), 7.60 (4H, t, J = 1.8 Hz, 4 × Ar**H**), 7.48–7.43 (2H, m, 2 × Ar**H**), 7.39–7.31 (4H, m, 4 × Ar**H**), 4.00 (8H, t, J = 7.1 Hz, 4 × C**H**$_2$), 3.78 (12H, s, 4 × C**H**$_3$), 2.11–2.01 (8H, m, 4 × C**H**$_2$), 1.56 (8H, app. quin, J = 7.3 Hz, 4 × C**H**$_2$), 1.11–1.03 (8H, m, 4 × C**H**$_2$), 1.02–0.93 (8H, m, 4 × C**H**$_2$), 0.64–0.45 (8H, m, 4 × C**H**$_2$) ppm; δ_C (100 MHz, DMSO-d_6) 151.0 (2 × **C**), 150.2 (2 × **C**), 140.2 (2 × **C**), 140.0 (2 × **C**), 139.2 (2 × **C**), 136.3 (4 × **C**H), 127.3 (2 × **C**H), 127.0 (2 × **C**H), 125.8 (2 × **C**H), 123.5 (4 × **C**H), 122.9 (2 × **C**H), 122.1 (4 × **C**H), 120.6 (2 × **C**H), 120.3 (2 × **C**H), 120.0 (2 × **C**H), 54.8 (2 × **C**), 48.7 (4 × **C**H_2), 39.3 (4 × **C**H_2), 35.7 (4 × **C**H_3), 29.3 (4 × **C**H_2), 28.8 (4 × **C**H_2), 25.4 (4 × **C**H_2), 23.5 (4 × **C**H_2) ppm; LRMS (ESI$^+$) 340 (100%, $[MH]^+$); LRMS (ESI$^+$) 248 (100%, $[M - 4 \times PF_6]^{4+}$).

2.1.2.4. 9,9,9′,9′-Tetrakis-(6-(1-methyl-3H-imidazolium-3-yl)hexyl)-9H,9′H-2,2′-bifluorene tetratriflate, ***4b****.* A solution of bifluorene **3** (235 mg, 0.24 mmol) and *N*-methylimidazole (0.081 mL, 1.01 mmol) in toluene (20 mL) was heated at 100 °C for 18 h then cooled to RT and concentrated *in vacuo*. The resulting solid was dissolved in acetone (10 mL) and 1 M CF_3SO_2K (1.0 M, 10 mL) added. After 5 min the solution was concentrated *in vacuo*, then the resulting solid was washed with H_2O (200 mL), dissolved in acetone (50 mL), concentrated *in vacuo*, washed with hexane (200 mL), dissolved in acetone (50 mL), concentrated *in vacuo* then sonicated as a suspension in $CHCl_3$ (250 mL) for 15 min. The filtrate was collected, washed with further $CHCl_3$ (200 mL) then twice dissolved in acetone (50 mL) and concentrated *in vacuo*, to afford the title compound **4b** as a pale yellow solid (350 mg, 0.23 mmol, 98%), δ_H (400 MHz, DMSO-d_6) 8.96 (4H, br s, 4 × Ar**H**), 7.89 (2H, d, J = 8.0 Hz, 2 × Ar**H**), 7.87–7.83 (4H, m, 4 × Ar**H**), 7.75 (2H, dd, J = 8.0, 1.5 Hz, 2 × Ar**H**), 7.63 (4H, t, J = 1.9 Hz, 4 × Ar**H**), 7.62 (4H, t, J = 1.9 Hz, 4 × Ar**H**), 7.48–7.44 (2H, m, 2 × Ar**H**), 7.39–7.31 (4H, m, 4 × Ar**H**), 4.00 (8H, t, J = 7.2 Hz, 4 × C**H**$_2$), 3.79 (12H, s, 4 × C**H**$_3$), 2.11–2.00 (8H, m, 4 × C**H**$_2$), 1.56 (8H, app. quin, J = 7.3 Hz, 4 × C**H**$_2$), 1.13–1.02 (8H, m, 4 × C**H**$_2$), 1.02–0.93 (8H, m, 4 × C**H**$_2$), 0.64–0.44 (8H, m, 4 × C**H**$_2$) ppm; δ_C (100 MHz, DMSO-d_6) 150.9 (2 × **C**), 150.2 (2 × **C**), 140.2 (2 × **C**), 140.0 (2 × **C**), 139.2 (2 × **C**), 136.3 (4 × **C**H), 127.3 (2 × **C**H), 127.0 (2 × **C**H), 125.8 (2 × **C**H), 123.5 (4 × **C**H), 122.9 (2 × **C**H), 122.1 (4 × **C**H), 120.7 (q, J = 322.1 Hz, 4 × **C**F_3), 120.6 (2 × **C**H), 120.3 (2 × **C**H), 120.0 (2 × **C**H), 54.8 (2 × **C**), 48.7 (4 × **C**H_2), 39.3 (4 × **C**H_2), 35.7 (4 × **C**H_3), 29.3 (4 × **C**H_2), 28.8 (4 × **C**H_2), 25.4 (4 × **C**H_2), 23.5 (4 × **C**H_2) ppm; δ_F (376 MHz, DMSO-d_6) −77.51 (s, 4 × C**F**$_3$) ppm; LRMS (ESI$^+$) 248 (100%, $[M - 4 \times CF_3SO_2]^{4+}$).

2.1.2.5. 9,9,9′,9′-Tetrakis-(6-(1-butyl-3H-imidazolium-3-yl)hexyl)-9H,9′H-2,2′-bifluorene tetrakis(hexafluorophosphate), ***4c****.* A solution of bifluorene **3** (271 mg, 0.28 mmol) and *N*-butylimidazole (144 mg, 1.16 mmol) in toluene (20 mL) was heated at 100 °C for 18 h then cooled to RT and concentrated *in vacuo*. The resulting solid was dissolved in acetone (10 mL) and 1 M KPF_6 (10 mL) added. After 5 min the solution was concentrated *in vacuo*, then the resulting solid was washed with water (200 mL), dissolved in acetone (50 mL), concentrated *in vacuo*, washed with hexane (200 mL), dissolved in acetone (50 mL), concentrated *in vacuo* then sonicated as a suspension in $CHCl_3$ (250 mL) for 15 min. The solid was collected by filtration then twice dissolved in acetone (50 mL) and concentrated *in vacuo* to afford the title compound **4c** as an off-white solid (441 mg, 0.24 mmol, 86%), δ_H (400 MHz, DMSO-d_6) 9.08 (4H, br s, 4 × Ar**H**), 7.89 (2H, d, J = 8.0 Hz, 2 × Ar**H**), 7.87–7.82 (4H, m, 4 × Ar**H**), 7.74 (2H, dd, J = 8.1, 1.5 Hz, 2 × Ar**H**), 7.72 (4H, t, J = 1.8 Hz, 4 × Ar**H**), 7.67 (4H, t, J = 1.8 Hz, 4 × Ar**H**), 7.47–7.43 (2H, m, 2 × Ar**H**), 7.39–7.30 (4H, m, 4 × Ar**H**), 4.11 (8H, t, J = 7.2 Hz, 4 × C**H**$_2$), 4.02 (8H, t, J = 7.2 Hz, 4 × C**H**$_2$), 2.11–1.99 (8H, m, 4 × C**H**$_2$), 1.72 (8H, app. quin, J = 7.3 Hz, 4 × C**H**$_2$), 1.58 (8H, app. quin, J = 7.3 Hz, 4 × C**H**$_2$), 1.19 (8H, app. quin, J = 7.3 Hz, 4 × C**H**$_2$), 1.11–1.02 (8H, m, 4 × C**H**$_2$), 1.02–0.93 (8H, m, 4 × C**H**$_2$), 0.85 (12H, t, J = 7.6 Hz, 4 × C**H**$_3$), 0.64–0.45 (8H, m, 4 × C**H**$_2$) ppm; δ_C (100 MHz, DMSO-d_6) 151.0 (2 × **C**), 150.2 (2 × **C**), 140.2 (2 × **C**), 140.0 (2 × **C**), 139.2 (2 × **C**), 136.3 (4 × **C**H), 127.3 (2 × **C**H), 127.0 (2 × **C**H), 125.8 (2 × **C**H), 123.5 (4 × **C**H), 122.9 (2 × **C**H), 122.1 (4 × **C**H), 120.6 (2 × **C**H), 120.3 (2 × **C**H), 120.0 (2 × **C**H), 54.8 (2 × **C**), 48.7 (4 × **C**H_2), 35.7 (4 × **C**H_2), 29.3 (4 × **C**H_2), 28.8 (4 × **C**H_2), 25.4 (4 × **C**H_2), 23.5 (4 × **C**H_2) ppm; LRMS (ESI$^+$) 290 (100%, $[M - 4 \times PF_6]^{4+}$).

2.1.2.6. 9,9,9′,9′-Tetrakis(6'-(3-butyl-1H-imidazolium)hexyl)-9H,9′H-2,2′-bifluorene tetratriflate, ***4d****.* A solution of bifluorene **3** (252 mg, 0.25 mmol) and *N*-butylimidazole (131 mg, 1.06 mmol) in toluene (20 mL) was heated at 100 °C for 18 h then cooled to RT and concentrated *in vacuo*. The resulting solid was dissolved in acetone (10 mL) and 1 M CF_3SO_2K (10 mL) added. After 5 min the solution was concentrated *in vacuo*, then the resulting solid was washed with hexane (200 mL), dissolved in acetone (50 mL) then sonicated as a suspension in $CHCl_3$ (250 mL) for 15 min. The solid was collected by filtration, washed with further $CHCl_3$ (200 mL) then twice dissolved in acetone (50 mL) and concentrated *in vacuo* to afford the title compound **4d** as an orange-brown gum (329 mg, 0.19 mmol, 77%), δ_H (400 MHz, DMSO-d_6) 9.08 (4H, br s, 4 × Ar**H**), 7.89 (2H, d, J = 8.0 Hz, 2 × Ar**H**), 7.86–7.82 (4H, m, 4 × Ar**H**), 7.74 (2H, dd, J = 8.1, 1.5 Hz, 2 × Ar**H**), 7.76–7.71 (6H, m, 6 × Ar**H**), 7.67 (4H, t, J = 1.7 Hz, 4 × Ar**H**), 7.47 - 7.42 (2H, m, 2 × Ar**H**), 7.39 - 7.30 (4H, m, 4 × Ar**H**), 4.11 (8H, t, J = 7.2 Hz, 4 × C**H**$_2$), 4.02 (8H, t, J = 7.0 Hz, 4 × C**H**$_2$), 2.11–1.99 (8H, m, 4 × C**H**$_2$), 1.72 (8H, app. quin, J = 7.3 Hz, 4 × C**H**$_2$), 1.58 (8H, app. quin, J = 7.2 Hz, 4 × C**H**$_2$), 1.19 (8H, app. q, J = 7.5 Hz, 4 × C**H**$_2$), 1.11–1.02 (8H, m, 4 × C**H**$_2$), 1.02–0.92 (8H, m, 4 × C**H**$_2$), 0.84 (12H, t, J = 7.4 Hz, 4 × C**H**$_3$) ppm; δ_C (100 MHz, DMSO-d_6) 150.9 (2 × **C**), 150.2 (2 × **C**), 140.2 (2 × **C**), 140.0 (2 × **C**), 139.2 (2 × **C**), 135.8 (4 × **C**H), 127.3 (2 × **C**H), 127.0 (2 × **C**H), 125.8 (2 × **C**H), 122.9 (2 × **C**H), 122.41 (4 × **C**H), 122.35 (4 × **C**H), 120.7 (q, J = 322.1 Hz, 4 × **C**F_3), 120.6 (2 × **C**H), 120.3 (2 × **C**H), 120.0 (2 × **C**H), 54.8 (2 × **C**), 48.8 (4 × **C**H_2), 48.6 (4 × **C**H_2), 39.3 (4 × **C**H_2), 31.2 (4 × **C**H_2), 29.2 (4 × **C**H_2), 28.8

(4 × **C**H_2), 25.4 (4 × **C**H_2), 23.5 (4 × **C**H_2), 18.7 (4 × **C**H_2), 13.2 (4 × **C**H_3) ppm; δ_F (376 MHz, DMSO-d_6) −77.52 (s, 4 × C**F_3**); LRMS (ESI^+) 290 (100%, $[M - 4 \times CF_3SO_2]^{4+}$).

2.1.2.7. 9,9′,9′-Tetrakis-(6-(1-hexyl-3H-imidazolium-3-yl)hexyl)-9H,9′H-2,2′-bifluorene tetrakis(hexafluorophosphate), ***4e****.* A solution of bifluorene **3** (256 mg, 0.26 mmol) and *N*-hexylimidazole (167 mg, 1.10 mmol) in toluene (20 mL) was heated at 100 °C for 18 h then cooled to RT and concentrated *in vacuo*. The resulting solid was dissolved in acetone (10 mL) and 1 M KPF_6 (10 mL) added. After 5 min the solution was concentrated *in vacuo*, then the resulting solid was washed with water (200 mL), dissolved in acetone (50 mL), concentrated *in vacuo*, washed with hexane (200 mL), dissolved in acetone (50 mL), concentrated *in vacuo* then sonicated as a suspension in $CHCl_3$ (250 mL) for 15 min. The solid was collected by filtration then twice dissolved in acetone (50 mL) and concentrated *in vacuo* to afford the title compound **4e** as an off-white solid (333 mg, 0.18 mmol, 69%), δ_H (400 MHz, DMSO-d_6) 9.04 (4H, t, J = 1.4 Hz, 4 × Ar**H**), 7.87 (2H, d, J = 8.0 Hz, 2 × Ar**H**), 7.85–7.80 (4H, m, 4 × Ar**H**), 7.73 (2H, dd, J = 8.0, 1.4 Hz, 2 × Ar**H**), 7.70 (4H, t, J = 1.7 Hz, 4 × Ar**H**), 7.64 (4H, t, J = 1.8 Hz, 4 × Ar**H**), 7.46–7.41 (2H, m, 2 × Ar**H**), 7.38–7.29 (4H, m, 4 × Ar**H**), 4.09 (8H, t, J = 7.2 Hz, 4 × C**H_2**), 4.01 (8H, t, J = 7.0 Hz, 4 × C**H_2**), 2.10–1.98 (8H, m, 4 × C**H_2**), 1.73 (8H, app. quin, J = 7.2 Hz, 4 × C**H_2**), 1.57 (8H, app. quin, J = 7.2 Hz, 4 × C**H_2**), 1.25–1.10 (24H, m, 12 × C**H_2**), 1.11–1.02 (8H, m, 4 × C**H_2**), 1.01–0.90 (8H, m, 4 × C**H_2**), 0.84–0.74 (12H, m, 4 × C**H_3**), 0.62–0.45 (8H, m, 4 × C**H_2**) ppm; δ_C (100 MHz, DMSO-d_6) 150.9 (2 × **C**), 150.2 (2 × **C**), 140.2 (2 × **C**), 140.0 (2 × **C**), 139.2 (2 × **C**), 135.8 (4 × **C**H), 127.3 (2 × **C**H), 127.0 (2 × **C**H), 125.8 (2 × **C**H), 122.9 (2 × **C**H), 122.4 (4 × **C**H), 122.3 (4 × **C**H), 120.6 (2 × **C**H), 120.2 (2 × **C**H), 120.0 (2 × **C**H), 54.8 (2 × **C**), 48.82 (4 × **C**H_2), 48.80 (4 × **C**H_2), 39.3 (4 × **C**H_2), 30.4 (4 × **C**H_2), 29.2 (4 × **C**H_2), 29.1 (4 × **C**H_2), 28.8 (4 × **C**H_2), 25.4 (4 × **C**H_2), 25.0 (4 × **C**H_2), 23.5 (4 × **C**H_2), 21.8 (4 × **C**H_2), 13.7 (4 × **C**H_3) ppm; LRMS (ESI^+) 318 (100%, $[M - 4 \times PF_6]^{4+}$).

2.1.2.8. 9,9,9′,9′-Tetrakis(6′-(3-hexyl-1H-imidazolium)hexyl)-9H,9′H-2,2′-bifluorene tetratriflate, ***4f****.* A solution of bifluorene **3** (232 mg, 0.24 mmol) and *N*-hexylimidazole (151 mg, 0.99 mmol) in toluene (20 mL) was heated at 100 °C for 18 h then cooled to RT and concentrated *in vacuo*. The resulting solid was dissolved in acetone (10 mL) and 1 M CF_3SO_2K (10 mL) added. After 5 min the solution was concentrated *in vacuo*, then the resulting solid was washed with hexane (200 mL), dissolved in acetone (50 mL), concentrated *in vacuo* then sonicated as a suspension in $CHCl_3$ (250 mL) for 15 min. The solid was collected by filtration, washed with further $CHCl_3$ (200 mL) then twice dissolved in acetone (50 mL) and concentrated *in vacuo* to afford the title compound **4f** as an off-white gum (289 g, 0.16 mmol, 67%), δ_H (400 MHz, DMSO-d_6) 9.07 (4H, t, J = 1.4 Hz, 4 × Ar**H**), 7.88 (2H, d, J = 7.8 Hz, 2 × Ar**H**), 7.86–7.80 (4H, m, 4 × Ar**H**), 7.75–7.70 (6H, m, 6 × Ar**H**), 7.67 (4H, t, J = 1.8 Hz, 4 × Ar**H**), 7.46–7.41 (2H, m, 2 × Ar**H**), 7.38–7.29 (4H, m, 4 × Ar**H**), 4.10 (8H, t, J = 7.1 Hz, 4 × C**H_2**), 4.02 (8H, t, J = 7.0 Hz, 4 × C**H_2**), 2.09–1.98 (8H, m, 4 × C**H_2**), 1.73 (8H, app. quin, J = 7.2 Hz, 4 × C**H_2**), 1.57 (8H, app. quin, J = 7.2 Hz, 4 × C**H_2**), 1.24–1.12 (24H, m, 12 × C**H_2**), 1.10–1.01 (8H, m, 4 × C**H_2**), 1.01–0.91 (8H, m, 4 × C**H_2**), 0.83–0.76 (12H, m, 4 × C**H_3**), 0.64–0.45 (8H, m, 4 × C**H_2**); δ_C (100 MHz, DMSO-d_6) 150.9 (2 × **C**), 150.2 (2 × **C**), 140.2 (2 × **C**), 140.0 (2 × **C**), 139.2 (2 × **C**), 135.8 (4 × **C**H), 127.3 (2 × **C**H), 127.0 (2 × **C**H), 125.8 (2 × **C**H), 122.9 (2 × **C**H), 122.40 (4 × **C**H), 122.35 (4 × **C**H), 120.7 (q, J = 322.1 Hz, 4 × **C**F_3), 120.6 (2 × **C**H), 120.2 (2 × **C**H), 120.0 (2 × **C**H), 54.7 (2 × **C**), 48.81 (4 × **C**H_2), 48.79 (4 × **C**H_2), 39.3 (4 × **C**H_2), 30.4 (4 × **C**H_2), 29.2 (4 × **C**H_2), 29.1 (4 × **C**H_2), 28.8 (4 × **C**H_2), 25.4 (4 × **C**H_2), 25.0 (4 × **C**H_2), 23.5 (4 × **C**H_2), 21.8 (4 × **C**H_2), 13.7 (4 × **C**H_3) ppm; δ_F (376 MHz, DMSO-d_6) −77.53 (s, 4 × C**F_3**); LRMS (ESI^+) 318 (100%, $[M - 4 \times CF_3SO_2]^{4+}$).

2.1.2.9. 9,9,9′,9′-Tetrakis-(6-(1-octyl-3H-imidazolium-3-yl)octyl)-9H,9′H-2,2′-bifluorene tetrakis(hexafluorophosphate), ***4g****.* A solution of bifluorene **3** (237 mg, 0.24 mmol) and *N*-octylimidazole (182 mg, 1.01 mmol) in toluene (20 mL) was heated at 100 °C for 18 h then cooled to RT and concentrated *in vacuo*. The resulting solid was dissolved in acetone (10 mL) and 1 M KPF_6 (10 mL) added. After 5 min the solution was concentrated *in vacuo*, then the resulting solid was washed with water (200 mL), dissolved in acetone (50 mL), concentrated *in vacuo*, washed with hexane (200 mL), dissolved in acetone (50 mL), concentrated *in vacuo* then sonicated as a suspension in $CHCl_3$ (250 mL) for 15 min. The solid was collected by filtration then twice dissolved in acetone (50 mL) and concentrated *in vacuo* to afford the title compound **4g** as an off-white solid (297 mg, 0.15 mmol, 63%), δ_H (400 MHz, DMSO-d_6) 9.03 (4H, br s, 4 × Ar**H**), 7.86 (2H, d, J = 8.0 Hz, 2 × Ar**H**), 7.79–7.84 (4H, m, 4 × Ar**H**), 7.72 (2H, dd, J = 8.1, 1.2 Hz, 2 × Ar**H**), 7.68 (4H, t, J = 1.7 Hz, 4 × Ar**H**), 7.63 (4H, t, J = 1.7 Hz, 4 × Ar**H**), 7.46–7.40 (2H, m, 4 × Ar**H**), 7.37–7.28 (4H, m, 4 × Ar**H**), 4.08 (8H, t, J = 7.1 Hz, 4 × C**H_2**), 4.01 (8H, br t, J = 7.0 Hz, 4 × C**H_2**), 2.10–1.97 (8H, m, 4 × C**H_2**), 1.72 (8H, app. quin, J = 7.2 Hz, 4 × C**H_2**), 1.57 (8H, app. quin, J = 7.1 Hz, 4 × C**H_2**), 1.27–1.10 (40H, m, 20 × C**H_2**), 1.09–1.01 (8H, m, 4 × C**H_2**), 1.00–0.91 (8H, m, 4 × C**H_2**), 0.81 (12H, br t, J = 6.9 Hz, 4 × C**H_3**), 0.63–0.44 (8H, m, 4 × C**H_2**) ppm; δ_C (100 MHz, DMSO-d_6) 151.0 (2 × **C**), 150.3 (2 × **C**), 140.3 (2 × **C**), 140.1 (2 × **C**), 139.3 (2 × **C**), 135.8 (4 × **C**H), 127.3 (2 × **C**H), 127.1 (2 × **C**H), 125.9 (2 × **C**H), 123.0 (2 × **C**H), 122.44 (4 × **C**H), 122.38 (4 × **C**H), 120.6 (2 × **C**H), 120.3 (2 × **C**H), 120.1 (2 × **C**H), 54.8 (2 × **C**), 48.93 (4 × **C**H_2), 48.89 (4 × **C**H_2), 39.3 (4 × **C**H_2), 31.2 (4 × **C**H_2), 29.3 (4 × **C**H_2), 29.2 (4 × **C**H_2), 28.8 (4 × **C**H_2), 28.5 (4 × **C**H_2), 28.3 (4 × **C**H_2), 25.44 (4 × **C**H_2), 25.39 (4 × **C**H_2), 23.6 (4 × **C**H_2), 22.1 (4 × **C**H_2), 14.0 (4 × **C**H_3) ppm; LRMS (ESI^+) 346 (100%, $[M - 4 \times PF_6]^{4+}$).

2.1.2.10. 9,9,9′,9′-Tetrakis(6′-(3-octyl-1H-imidazolium)hexyl)-9H,9′H-2,2′-bifluorene tetratriflate, ***4h****.* A solution of bifluorene **3** (520 mg, 0.24 mmol) and *N*-octylimidazole (400 mg, 2.22 mmol) in toluene (20 mL) was heated at 100 °C for 18 h then cooled to RT and concentrated *in vacuo*. The resulting solid was dissolved in acetone (10 mL) and 1 M CF_3SO_2K (10 mL) added. After 5 min the solution was concentrated *in vacuo*, then the resulting solid was washed with hexane (200 mL), dissolved in acetone (50 mL), concentrated *in vacuo* then sonicated as a suspension in $CHCl_3$ (250 mL) for 15 min. The solid was collected by filtration, washed with further $CHCl_3$ (200 mL) then twice dissolved in acetone (50 mL) and concentrated *in vacuo* to afford the title compound **4h** as a white solid (499 mg, 0.16 mmol, 49%), δ_H (400 MHz, DMSO-d_6) 9.06 (4H, br. s, 4 × Ar**H**), 7.64 (6H, dt, J = 14.9, 8.0 Hz, 6 × Ar**H**), 7.75–7.70 (6H, m, 6 × Ar**H**), 7.68–7.65 (4H, m, 4 × Ar**H**), 7.43 (2H, br. d, J = 6.5 Hz, 2 × Ar**H**), 7.39–7.28 (4H, m, 4 × Ar**H**), 4.09 (8H, t, J = 7.1 Hz, 4 × C**H_2**), 4.02 (8H, br. t, J = 7.0 Hz, 4 × C**H_2**), 2.09–1.99 (8H, m, 4 × C**H_2**), 1.73 (8H, app. quin, J = 7.2 Hz, 4 × C**H_2**), 1.57 (8H, app. quin, J = 7.1 Hz, 4 × C**H_2**), 1.27–1.11 (40H, m, 20 × C**H_2**), 1.10–1.01 (8H, m, 4 × C**H_2**), 1.01–0.91 (8H, m, 4 × C**H_2**), 0.82 (12H, br. t, J = 6.9 Hz, 4 × C**H_3**), 0.65–0.44 (8H, m, 4 × C**H_2**); δ_C (100 MHz, DMSO-d_6) 150.9 (2 × **C**), 150.2 (2 × **C**), 140.2 (2 × **C**), 139.9 (2 × **C**), 139.2 (2 × **C**), 135.8

(4 × **C**H), 127.2 (2 × **C**H), 127.0 (2 × **C**H), 125.8 (2 × **C**H), 122.8 (2 × **C**H), 122.4 (4 × **C**H), 122.3 (4 × **C**H), 120.7 (q, J = 322.1 Hz, 4 × **C**F_3), 120.5 (2 × **C**H), 120.2 (2 × **C**H), 120.0 (2 × **C**H), 54.7 (2 × **C**), 48.80 (4 × **C**H_2), 48.76 (4 × **C**H_2), 39.5 (4 × **C**H_2), 31.1 (4 × **C**H_2), 29.21 (4 × **C**H_2), 29.15 (4 × **C**H_2), 28.9 (4 × **C**H_2), 28.4 (4 × **C**H_2), 28.2 (4 × **C**H_2), 25.4 (4 × **C**H_2), 25.3 (4 × **C**H_2), 23.5 (4 × **C**H_2), 22.0 (4 × **C**H_2), 13.9 (4 × **C**H_3) ppm; δ_F (376 MHz, DMSO-d_6) −77.52 (s, 4 × **C**$\mathbf{F_3}$); LRMS (ESI$^+$) 346 (100%, [M − 4 × CF_3SO_2]$^{4+}$).

2.2. Device fabrication and measurement

All the spray coating steps were performed under ambient atmospheric conditions. Nitrogen (N_2) gas was used to pressurise the pneumatic spray coating system. The distance from the nozzle to the substrate for spray coating was 15 cm, for both PEDOT:PSS and active layer deposition, with a differential inlet/outlet pressure of 0.3 bar. The glass slides were rinsed with deionized water and acetone in sequence to remove any surface contamination prior to functional coating. Fig. 2 (a) shows the isometric diagram of the OLEC device structure used in this research. A plan view photograph of a set of fabricated OLECs on a glass slide is shown in Fig. 2b. A PEDOT:PSS suspension in water was first spray coated directly on the ITO patterned substrate and annealed at 120 °C for 20 min in a conventional box oven.

Molecule **4a** was dissolved in acetonitrile at a concentration of 0.25 g/mL, and molecule **4h** was dissolved in ethanol at a concentration of 0.7 g/mL, to form the two active inks. The UV emitting active layer was spray coated in an ambient environment. However, the use of **4a** in the acetonitrile resulted in clogging of the spray nozzle after a few seconds. This can be attributed to its lower solubility as, during spray coating, compressed N_2 travels through the nozzle leading to an increase in the ink pressure. In turn, this cools the ink and reduces the solubility of the active component **4a** such that it precipitates out. The modified ink, based on analogue **4h**, did not lead to nozzle clogging and showed improved processing capability due to its high solubility in ethanol. Annealing of the spray coated active layer was undertaken at 70 °C over 5 h in a nitrogen filled box oven. To complete UV OLEC fabrication, a silver top electrode was sputter coated through a pre-defined shadow mask, by a coating current of 70 mA. The top electrode mask was pre-defined to achieve three light emitting pixels. Silver conductive paint was subsequently applied to establish contact points for testing. Finally, the device was encapsulated by drop casting an epoxy formulation onto the surface and covering with a coverslip. The fully encapsulation system was then UV cured with a 365 nm wavelength mercury lamp.

The following equipment was used: Field Emission Scanning Electron Microscopy (FESEM, JSM 7500F) manufactured by JEOL to take the cross-sectional SEM image of the UV OLEC devices to evaluate the functional layers' thickness. A UV/Vis/NIR (Cary 500) Spectrometer manufactured by Varian was used for UV/VIS transmission and absorption measurement. A high-speed sputter coater machine (Safematic CCU 010) was used for the top electrode deposition. UV/Vis/NIR spectroradiometer (Stellar-RAD 250–1100 nm) was used to measure the LECs UV emission intensity and spectrum. A 340 nm laser M340L4 (53 mW (Min), 700 mA) Mounted LED is supplied by Thorlabs, was used as the laser source for photoluminescence (PL) emission excitation. An adjustable Collimation Adapter (SM2F32-A) with Ø2″ Lens and AR Coating with a wavelength of 350–700 nm was used with a 340 nm laser source for PL measurements. UV OLEC devices fabricated on ITO pre-coated glass slide substrates were measured via the bottom emission to determine their EL spectrum. Absorption and PL measurements were performed on both solution state (using a cuvette) and a spray coated film. A sample of coated film on the glass substrate had a UV emitting film thickness of 250 nm. The absorption peak of the material indicates the range of optical source wavelengths which are necessary to carry out the PL measurement; the PL is excited by an optical source within the range of wavelengths identified in the absorption peak spectra. However, any wavelength below the absorption peak value will be able to excite PL emission.

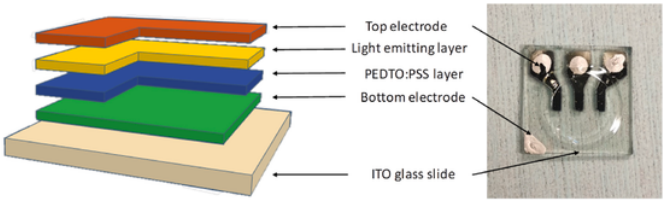

Fig. 2. (a) Schematic drawing of the spray coated UV-LECs on glass substrate and (b) plane view of the fabricated LECs.

3. Results and discussion

Our study was inspired by the work of Chen et al. [31] who had shown that 2,2′-bifluorene **4a** could be fabricated into an effective UV light-emitting electrochemical cell with good charge carrier mobilities and electrochemical properties. Unfortunately, for our purposes its poor solubility in many solvents proved limiting as it led to nozzle blockage during spray coating. To address this deficiency, we decided to examine the influence on solubility of both the counter ion and the nature of the alkyl residues on the imidazolium units. Thus, our target became the series of 2,2′-bifluorene **4b-h**, with methyl, *n*-butyl, *n*-hexyl and *n*-octyl imidazolium units, and either triflate or hexafluorophosphate counter ions. Each synthesis began with the *bis*-alkylation of 2-bromo-9*H*-fluorene **1** with 1,6-dibromohexane (Scheme 1). Dimerisation of the resulting tribromide **2** was next accomplished using a Suzuki–Miyaura coupling to give the lynchpin 2,2′-bifluorene **3** from which all of the targets **4a-h** could be synthesised through coupling with the appropriate imidazole, followed by ion exchange. Higher material losses were witnessed during purification of the higher homologues in this series, leading to a reduction in yield for these products. As expected, the incorporation of higher alkyl chains led to improved solubility in both ethanol and acetonitrile, as did the use of the triflate counter ion. Therefore, in this study, the known bifluorene **4a** and its derivative **4h** were used for OLEC device fabrication.

Fig. 3 a, b and c show a light transmittance of more than 85% through an empty cuvette, plain glass, and quartz slides, respectively. Optical absorption and PL measurements of UV emitters **4a** and **4h** were performed on solution state and spray coated film. Fig. 3d shows the wavelength of the 340 nm laser excitation which has been used to measure PL for UV emitters **4a** and **4h** separately. The optical absorption spectra of UV emitter **4a** shows the maximum absorption at 344 nm for the solution and 342 nm for the film state (Fig. 4a and b).

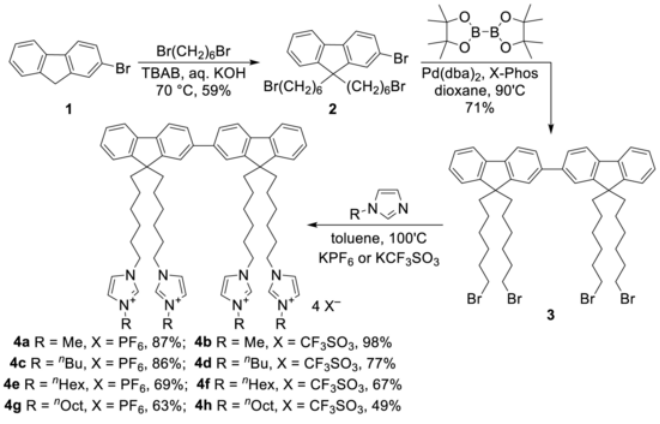

Scheme 1. Synthesis of the active bifluorenes **4a-h**.

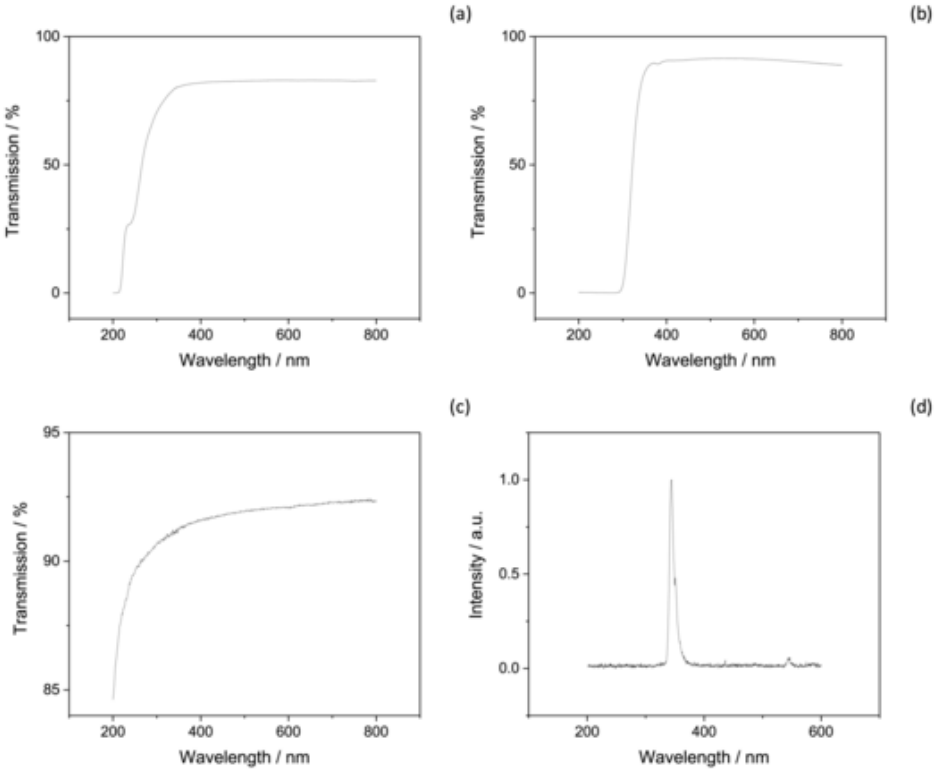

Fig. 3. Transmittance graph for empty cuvette, glass slides, quartz slides and the light source intensity of 340 nm reference laser for PL measurement.

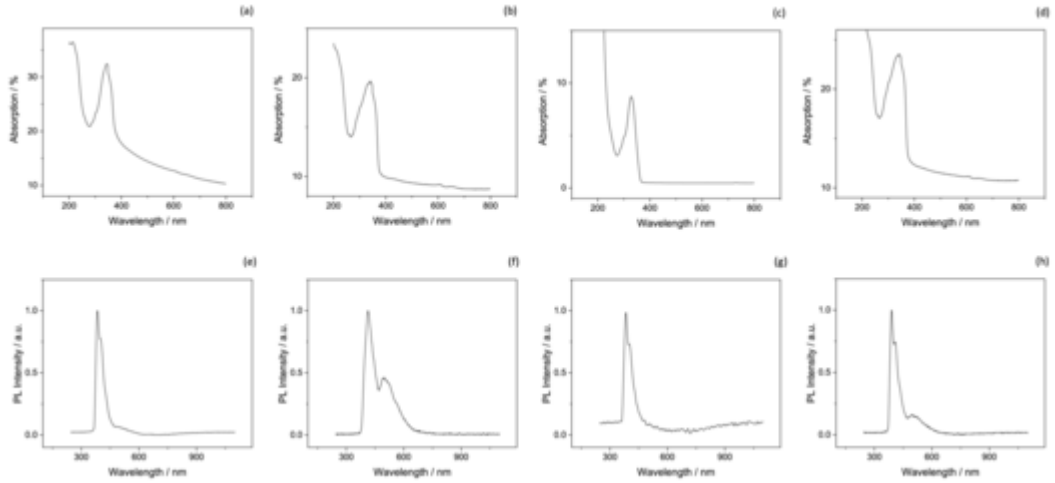

Fig. 4. Absorption measurements for solution (a) and spray coated film (b) state for UV emitter **4a**, and solution (c) and spray coated film (d) state for UV emitter **4h**; PL measurements for solution (e) and spray coated film (f) state for UV emitter **4a**, and PL measurements for solution (g) and spray coated film (h) state for UV emitter **4h**.

Fig. 4e and f shows PL spectra for the solution and spray coated film for **4a**, with an intense UV emission peak at 384 nm for the solution and 372 nm for the film state. The same trend is observed for **4h** in both the optical absorption and PL emission measurements as shown in Fig. 4c, d, g, and h. The absorption of **4h** is observed at 329 nm for the solution and 340–343 nm for the film state, while PL emission is observed at 383 nm for solution and 388 nm for the film state. This can be attributed to the common bifluorene UV core. Notably, the film state PL spectra of **4a** and **4h** (Fig. 4f and h) each display a second prominent peak at ~500 nm that is barely evident in the corresponding solution phase spectra (Fig. 4e and g). Moreover, the effect is more marked for **4a** than it is for **4h**. This observation suggests that aggregation plays a critical role in promoting these additional emission bands as the effect is greatest in the solid state and less pronounced when the imidazolium residues bare longer alkyl chains that disrupt aggregation [33].

Fig. 5a and d shows the FESEM images of the fabricated OLECs based on **4a** (Fig. 5a) and **4h** (Fig. 5d) on an ITO glass substrate. In both FESEM images, it can be observed that a 100 nm thick PEDOT:PSS film on top of a 300 nm ITO glass substrate. The OLEC active layer consisting of UV emitters **4a** and **4h** shows the thickness of 250 nm to achieve an intense emission as it was optimized in the PL film measurements. This indicates the UV emission **4h** with ethanol solvent formed a more interconnected film and has better spray coating reliability with triflate salts. As can be seen from the FESEM image in

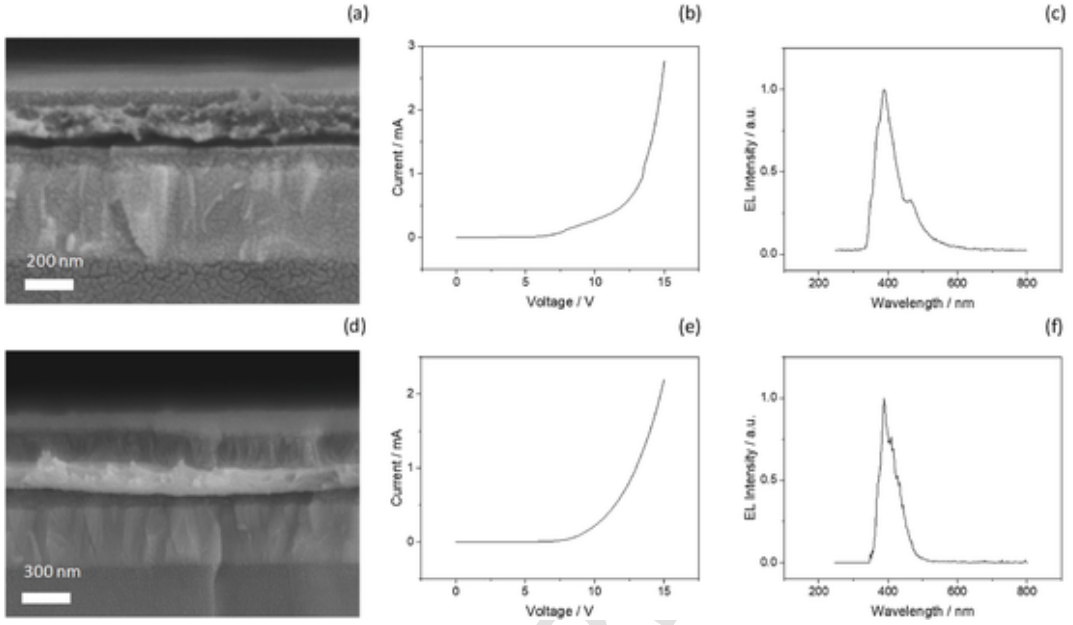

Fig. 5. FESEM image for (a) UV emitters **4a** and (d) **4h**, bottom to top, Glass substrate, 400 nm thick ITO layer, spray coated 100 nm PEDOT:PSS layer, 200 nm thickness UV emission OLEC layer, 100 nm silver top electrode; Current and Voltage sweep (I/V) curve for UV emitters (b) unencapsulated and (e) encapsulated devices. Electroluminescent (EL) spectrum of spray coated OLECs on pre-coated ITO glass slides with (c) **4a**, (f) **4h**.

Fig. 5d, for **4h,** a homogenous film with no porous texture is observed. In contrast, some degree of porosity in the active layer is observed for the UV emitter **4a,** as shown in Fig. 5a. Then, the active layer was followed by a 100 nm silver layer as the top electrode. The devices, fabricated using both **4a** and **4h**, were then subjected to the UV light emission by sweeping the voltage between 0 V–15 V. The 1 μm thick encapsulation layer deposited to protect the devices is not shown in the FESEM image. The I/V plots, as shown in Fig. 5b and e, demonstrate a 6.5 V turn on voltage for both **4a** and **4h** devices. As the new molecule **4h** reported here could effectively emit UV light in both solution and spray coated solid state film, this research work was extended further to investigate its EL performance.

Fig. 5c and f shows the EL spectrum plots captured under electrical bias at 10 V voltage, resulting in the maximum emission intensity. Fig. 5c and f shows the light emitting at a broader range of wavelengths than the obtained PL spectrum. Fig. 5c shows the fabricated **4a** EL emission starts from 360 nm towards 480 nm, with a peak at 385 nm and a secondary broad peak covering 415–430 nm; however, strong emission is recorded between 370 nm and 480 nm. Table 1 summarises the UV OLEC devices' key characteristics captured and derived from the measurement data from both **4a** and **4h** molecules. Emission intensity of **4a** is captured at the peak wavelength under 10 V bias, ~1.29 μW/cm^2. Fig. 5f shows the fabricated **4h** EL emission starts from 360 nm to 445 nm with a peak at 388–390 nm and a secondary peak at 409 nm. Emission intensity of ~0.86 μW/cm^2 of **4h** is captured at the peak wavelength under 10 V bias. However, strong emission is recorded between 370 nm and 430 nm. The current density of **4a** cells is slightly higher which leads to the higher intensity emission, comparing to the **4h** cells. However, **4h** cells demonstrate better stability and lifetime, compared to 4a cells. The variation between the two EL spectrum plots could be caused by the advancing of the salt system, which was initially designed to increase its solubility and widen its compatibility with more environmentally friendly solvent systems. Although the alkyl chains are introduced to achieve good processability, the UV emission intensity value of **4h** was lower than for **4a**. This might be due to the bulky alkyl chains that disturb the closely packed aromatic backbone planarity. It is important that the selection of alkyl chains improve solubility but does not disturb the conjugated planarity that might lead to high charge carrier transport in the conjugated backbone [34]. Even though the devices lifetimes are short, both molecules demonstrated that they are capable of UV emission and can be utilized to fabricate UV OLEC devices.

Table 1
Summary of the UV OLEC devices' key characteristics.

Device	Molecule	EL Peak (nm)	V_{on} (V)	V_{bias} (V)	J_{max} (mA/cm^2)	L_{max} (μW/cm^2)	Lifetime (min)[a]
I	4a	386	6.5	10	14	1.29	0.9
II	4h	388	6.5	10	10.5	0.86	1.3

[a] The time for the light output of the device to decay from the maximum to 30% of the maximum under a constant bias voltage of 10 V.

The **4a** and **4h** devices were subjected to increased voltage up to 15 V until the active layer failed to operate. The devices survived up to 12 V for 30 s but less than 5 s when biased at 15 V and no response was observed when the voltage increased beyond 15 V. The intensity value of the **4a** and **4h** cells reach around 8–10 μW/cm^2 at 15 V bias voltage, however, the lifetime is too short for the cells to observe the emission. In addition to that, it is necessary to study the solution processing of the inverted OLEC structure to enable the OLEC to be realized on textile substrates. The inverted structure means the light is emitted from the top surface of the OLECs and this is essential for the textile substrate which does not allow bottom emission. The key challenge is to use solution processing to deposit suitable patterned transparent/translucent top electrodes that enable the top emission.

4. Conclusions

We have prepared bifluorene derivatives **4a-h** and identified an improved solubility regime for **4h**. We have also utilized two different counter ions such as PF_6^- and $CF_3SO_3^-$ to improve the device performance. All the functional layers have been deposited by spray coating to afford working UV OLEC devices. Based on UV/Vis absorption and PL intensity plots, the encapsulation of the devices has been successfully demonstrated with a turn on voltage of 6.5 V. Finally, the presented work demonstrates novel ideas for chemists in design and modified synthesis of advanced UV light emitting materials with the salts for OLEC applications. This reported fabrication method can also be

adapted in use of large area electronics manufacturing of light emitting textiles. Future work will be focused on EL, flexibility and stability of the printed OLECs. The devices will also be prepared on textile substrates to demonstrate UV emitting textile OLECs.

Declaration of competing interest

The authors declare the following financial interests/personal relationships which may be considered as potential competing interests: Sasikumar Arumguam reports financial support was provided by University of Southampton. Sasikumar Arumugam reports a relationship with University of Southampton that includes: employment and funding grants.

Acknowledgements

The authors would like to thank the Engineering and Physical Sciences Research Council (EPSRC) for funding EP/S005307/1 (Functional electronic textiles for light emitting and colour changing applications) and EP/K039466/1 (Core Capability for Chemistry Research in Southampton), and European Regional Development Fund (ERDF) for funding InterReg V project 208 (SmartT: Smart Textiles for Regional Industry and Smart Specialisation Sectors). The work of Steve Beeby was supported by the Royal Academy of Engineering under the Chairs in Emerging Technologies Scheme. All data supporting this study are openly available from the University of Southampton repository at https://doi.org/10.5258/SOTON/D2148.

References

[1] S. Kwon, W. Kim, H. Kim, S. Choi, B.-C. Park, S.-H. Kang, K.C. Choi, High luminance fiber-based polymer light-emitting devices by a dip-coating method, Adv. Electron. Mater. 1 (2015) 1500103.
[2] H.L. Wainwright, 9 - design, evaluation, and applications of electronic textiles** Inventor of LED/Optic Fabric Displays, received over a dozen patents in the E-Textile applications and manufacturing sectors, Technology Consultant to fashion designers including the late Alexander McQueen for creating E-Textile fashions. Award Winner: NASA's "Design the Future" contest with E-Textile application, Guest Speaker at Flexible Display, Smart Fabric, Textile, and LED conferences, in: L. Wang (Ed.), Performance Testing of Textiles, Woodhead Publishing, 2016, pp. 193–213.
[3] D. Janczak, M. Zych, T. Raczyński, Ł. Dybowska-Sarapuk, A. Pepłowski, J. Krzemiński, A. Sosna-Głębska, K. Znajdek, M. Sibiński, M. Jakubowska, Stretchable and washable electroluminescent display screen-printed on textile, Nanomaterials (Basel) 9 (2019) 1276.
[4] A. Martin, A. Fontecchio, Effect of fabric integration on the physical and optical performance of electroluminescent fibers for lighted textile applications, Fibers 6 (2018) 50.
[5] B. Hu, D. Li, O. Ala, P. Manandhar, Q. Fan, D. Kasilingam, P.D. Calvert, Textile-based flexible electroluminescent devices, Adv. Funct. Mater. 21 (2011) 305–311.
[6] M. de Vos, R. Torah, J. Tudor, Dispenser printed electroluminescent lamps on textiles for smart fabric applications, Smart Mater. Struct. 25 (2016) 045016.
[7] Q. Pei, G. Yu, C. Zhang, Y. Yang, A.J. Heeger, Polymer light-emitting electrochemical cells, Science 269 (1995) 1086–1088.
[8] S. Tang, L. Edman, Light-emitting electrochemical cells: a review on recent progress, Top. Curr. Chem. 374 (2016) 40.
[9] S.B. Meier, D. Tordera, A. Pertegás, C. Roldán-Carmona, E. Ortí, H.J. Bolink, Light-emitting electrochemical cells: recent progress and future prospects, Mater. Today 17 (2014) 217–223.
[10] S. Kanagaraj, A. Puthanveedu, Y. Choe, Small Molecules in Light-Emitting Electrochemical Cells: Promising Light-Emitting Materials, Advanced Functional Materials, n/a 1907126.
[11] E. Nannen, J. Frohleiks, S. Gellner, Light-emitting electrochemical cells based on color-tunable inorganic colloidal quantum dots, Adv. Funct. Mater., n/a 1907349.
[12] Q. Sun, Y. Li, Q. Pei, Polymer light-emitting electrochemical cells for high-efficiency low-voltage electroluminescent devices, J. Disp. Technol. 3 (2007) 211–224.
[13] M. Di Marcantonio, J.E. Namanga, V. Smetana, N. Gerlitzki, F. Vollkommer, A.V. Mudring, G. Bacher, E. Nannen, Green-yellow emitting hybrid light emitting electrochemical cell, J. Mater. Chem. C 5 (2017) 12062–12068.
[14] T. Sajoto, P.I. Djurovich, A. Tamayo, M. Yousufuddin, R. Bau, M.E. Thompson, R.J. Holmes, S.R. Forrest, Blue and near-UV phosphorescence from iridium complexes with cyclometalated pyrazolyl or N-heterocyclic carbene ligands, Inorg. Chem. 44 (2005) 7992–8003.
[15] J. Frohleiks, S. Gellner, S. Wepfer, G. Bacher, E. Nannen, Design and realization of white quantum dot light-emitting electrochemical cell hybrid devices, ACS Appl. Mater. Interfaces 10 (2018) 42637–42646.
[16] C.-M. Wang, Y.-M. Su, T.-A. Shih, G.-Y. Chen, Y.-Z. Chen, C.-W. Lu, I.-S. Yu, Z.-P. Yang, H.-C. Su, Achieving highly saturated single-color and high color-rendering-index white light-emitting electrochemical cells by CsPbX3 perovskite color conversion layers, J. Mater. Chem. C 6 (2018) 12808–12813.
[17] A.F. Henwood, E. Zysman-Colman, Luminescent iridium complexes used in light-emitting electrochemical cells (LEECs), Top. Curr. Chem. (Cham) 374 (2016), 36-36.
[18] A. Sandström, H.F. Dam, F.C. Krebs, L. Edman, Ambient fabrication of flexible and large-area organic light-emitting devices using slot-die coating, Nat. Commun. 3 (2012) 1002.
[19] T. Lanz, A. Sandström, S. Tang, P. Chabrecek, U. Sonderegger, L. Edman, A light–emission textile device: conformal spray-sintering of a woven fabric electrode, Flex. Print. Electron. 1 (2016) 025004.
[20] S. Tang, L. Edman, Quest for an appropriate electrolyte for high-performance light-emitting electrochemical cells, J. Phys. Chem. Lett. 1 (2010) 2727–2732.
[21] S. Tang, W.-Y. Tan, X.-H. Zhu, L. Edman, Small-molecule light-emitting electrochemical cells: evidence for in situ electrochemical doping and functional operation, Chem. Commun. 49 (2013) 4926–4928.
[22] Y. Choe, C.D. Sunesh, M.S. Subeesh, K. Shanmugasundaram, Small molecule-based light-emitting electrochemical cells, in: R.D. Costa (Ed.), Light-Emitting Electrochemical Cells: Concepts, Advances and Challenges, Springer International Publishing, Cham, 2017, pp. 329–349.
[23] J. Park, K. Shanmugasundaram, J.C. John, Y. Choe, Aggregation induced emission small molecules for blue light-emitting electrochemical cells, J. Photochem. Photobiol. Chem. 374 (2019) 10–15.
[24] H. Lee, C.D. Sunesh, M.S. Subeesh, Y. Choe, Blue-light emitting electrochemical cells comprising pyrene-imidazole derivatives, Opt. Mater. 78 (2018) 44–51.
[25] J. Mindemark, L. Edman, Illuminating the electrolyte in light-emitting electrochemical cells, J. Mater. Chem. C 4 (2016) 420–432.
[26] K. Youssef, Y. Li, S. O'Keeffe, L. Li, Q. Pei, Fundamentals of materials selection for light-emitting electrochemical cells, Adv. Funct. Mater. 30 (2020) 1909102.
[27] K. Matsuki, J. Pu, T. Takenobu, Recent progress on light-emitting electrochemical cells with nonpolymeric materials, Adv. Funct. Mater. 30 (2020) 1908641.
[28] H. Luo, L. Zhong, Ultraviolet germicidal irradiation (UVGI) for in-duct airborne bioaerosol disinfection: review and analysis of design factors, Build. Environ. 197 (2021) 107852.
[29] S. Arumugam, Y. Li, J. Pearce, M.D.B. Charlton, J. Tudor, D. Harrowven, S. Beeby, Visible and ultraviolet light emitting electrochemical cells realised on woven textiles, Proceedings 68 (2021) 9.
[30] Y. Li, N. Grabham, A. Komolafe, J. Tudor, Battery free smart bandage based on NFC RFID technology, in: IEEE International Conference on Flexible and Printable Sensors and Systems (FLEPS)2020, 2020, pp. 1–4.
[31] H.-F. Chen, C.-T. Liao, M.-C. Kuo, Y.-S. Yeh, H.-C. Su, K.-T. Wong, UV light-emitting electrochemical cells based on an ionic 2,2′-bifluorene derivative, Org. Electron. 13 (2012) 1765–1773.
[32] Y. Li, S. Arumugam, C. Krishnan, M.D.B. Charlton, S.P. Beeby, Encapsulated textile organic solar cells fabricated by spray coating, ChemistrySelect 4 (2019) 407–412.
[33] L. Sun, N. Sun, L. Bai, X. An, B. Liu, C. Sun, L. Fan, C. Wei, Y. Han, M. Yu, J. Lin, D. Lu, N. Wang, L. Xie, K. Shen, X. Zhang, Y. Xu, J. Cabanillas-Gonzalez, W. Huang, Alkyl-chain branched effect on the aggregation and photophysical behavior of polydiarylfluorenes toward stable deep-blue electroluminescence and efficient amplified spontaneous emission, Chin. Chem. Lett. 30 (2019) 1959–1964.
[34] Y. Che, D.F. Perepichka, Quantifying planarity in the design of organic electronic materials, Angew. Chem. Int. Ed. 60 (2021) 1364–1373.